Submitted to Physics of Fluids

UCRL-19635
Preprint

c.2

THE EFFECT OF CONDENSATION IN THE BOUNDARY LAYER ON MASS TRANSFER FROM A ROTATING DISK

PART I - THEORETICAL

RECEIVED
LAWRENCE
RADIATION LABORATORY

JUL 21 1970

LIBRARY AND
DOCUMENTS SECTION

R. P. Omberg and D. R. Olander

June 1970

AEC Contract No. W-7405-eng-48

TWO-WEEK LOAN COPY

This is a Library Circulating Copy which may be borrowed for two weeks. For a personal retention copy, call Tech. Info. Division, Ext. 5545

UCRL-19635
cy 2

LAWRENCE RADIATION LABORATORY
UNIVERSITY of CALIFORNIA · BERKELEY

DISCLAIMER

This document was prepared as an account of work sponsored by the United States Government. While this document is believed to contain correct information, neither the United States Government nor any agency thereof, nor the Regents of the University of California, nor any of their employees, makes any warranty, express or implied, or assumes any legal responsibility for the accuracy, completeness, or usefulness of any information, apparatus, product, or process disclosed, or represents that its use would not infringe privately owned rights. Reference herein to any specific commercial product, process, or service by its trade name, trademark, manufacturer, or otherwise, does not necessarily constitute or imply its endorsement, recommendation, or favoring by the United States Government or any agency thereof, or the Regents of the University of California. The views and opinions of authors expressed herein do not necessarily state or reflect those of the United States Government or any agency thereof or the Regents of the University of California.

THE EFFECT OF CONDENSATION IN THE BOUNDARY LAYER ON MASS TRANSFER FROM A ROTATING DISK

PART I - THEORETICAL

R.P. Omberg* and D.R. Olander

Department of Nuclear Engineering
University of California

and the

Inorganic Materials Research Division
Lawrence Radiation Laboratory
Berkeley, California

ABSTRACT

When vaporization occurs in the presence of a temperature gradient in the boundary layer, homogeneous nucleation and condensation of droplets may occur. This process is studied theoretically in a rotating disk flow system for iron vaporizing into an atmosphere of cold argon. The usual boundary layer conservation equations are provided with appropriate source or sink terms to account for the conversion of the gaseous diffusing species (monomer) to drops of liquid and vice versa. Conservation equations for the monomer and for drops of all sizes are required. The source and sink terms are developed from the classical theory of homogeneous nucleation. Simultaneous solution of the coupled monomer and droplet equations provides insight into the enhancement of the vaporization rate due to condensation and also into the structure of the nucleation, droplet growth, and re-evaporation cycle which were found to take place in the boundary layer on the disk.

*Present address: Battelle Northwest Laboratory
Battelle Memorial Institute
Richland, Washington

I. INTRODUCTION

The vaporization rate of a hot surface into a cold gas environment may be substantially increased above the diffusion-limited value if the vaporizing species condenses in the thermal boundary layer. When condensation does occur, the diffusing molecules combine to form drops in accordance with the laws of nucleation kinetics. The creation of drops produces a sink in the ordinary convective-diffusion process which depresses the vapor pressure profile and causes an increase in the gradient at the wall. Hence, a larger vaporization rate is obtained.

Turkdogan[1] has investigated this enhancement in the vaporization rate for molten iron spheres in helium. He used the concept of the "critical supersaturation" from classical infinite-medium nucleation kinetics, which shows that if the supersaturation is above the "critical" value, condensation takes place at an extremely rapid rate; if the supersaturation is below the critical value, condensation takes place at an extremely slow rate.[2-8] In Turkdogan's analysis, the boundary layer was divided into two distinct zones: a condensate-free region close to the vaporizing surface in which the supersaturation is less than the critical value and an outer portion in which sufficient condensation occurs to maintain the supersaturation at the critical value corresponding to the

local gas temperature. The profile between the condensation zone and the wall was assumed to be linear, as in the stagnant film model of ordinary mass transfer. The theoretical results agreed qualitatively with a limited amount of rough experimental data taken by Turkdogan and Mills,[9] which indicated the enhancement in the vaporization rate to be approximately a factor of three.

With the additional assumption that the logarithm of the critical supersaturation was a linear function of the reciprocal temperature, Rosner[10] developed a set of analytical relationships to describe Turkdogan's model.

The major assumptions of the critical supersaturation approach are:

(1) Mass transfer is based upon the stagnant film model. In particular, drops formed in the outer condensing region of the boundary layer are not convected into the wall region, which is assumed to be free of drops larger than critical size.

(2) The location of the nucleation zone is determined by a critical supersaturation value obtained from the infinite-medium solution of the nucleation kinetic equations for an arbitrarily selected nucleation rate.

(3) The drop temperature is equal to the local gas temperature. Thermal radiation from the hot wall to the drop is neglected.

(4) Diffusion of the drops is neglected. Only the vapor species (the "monomer") diffuses. Elenbaas[11]

has shown that if drops do not penetrate the outer edge of the boundary layer, drop diffusion eliminates enhancement of the vaporization rate in the stagnant film model.

Epstein and Rosner[12] have examined the validity of the second assumption of the critical supersaturation model by simultaneously solving the classical nucleation equations (the infinite medium solution) with the conservation equations for a stagnant film mass transfer situation. Their analysis contains a convective term caused by the interfacial velocity which transports drops away from the vaporizing surface. As a result, drops leave the outer edge of the film and acceleration of the vaporization rate occurs. For this stagnant film model, Epstein and Rosner suggest that drop diffusion is unimportant.

Epstein and Rosner also found that nucleation currents in the boundary layer were on the order of 10^{10} to 10^{14} drops/cm^3-sec rather than the figure of 1 drop/cm^3-sec which is commonly used to define the critical supersaturation in cloud chambers[2-8] and in boundary layers.[9,10] A current of 1 drop/cm^3-sec is easily countable by visual techniques in cloud chambers. Its use to define the critical supersaturation in boundary layers is simply an <u>ad hoc</u> assumption. The actual nucleation current in a boundary layer is, in fact, determined by a mass balance between the drops and the vapor.

The approach of Epstein and Rosner is similar to that used in the analysis of condensation in expansion nozzles.[13,14]

In this approach, droplets are nucleated at rates dependent upon the local supersaturation in accordance with classical nucleation theory. These embryos are then convected along flow streamlines and grow by absorbing vapor from the surrounding gas phase. This method is Lagrangian in flavor, since the characteristics of the drop population at any point in the one-dimensional flow field are determined by integration of the growth history of the drops from their upstream nucleation point. In mass transfer problems, this approach is convenient if the direction of the mass transfer and flow streamlines coincide, as is the case in the stagnant film model analyzed by Epstein and Rosner. However, for many flow geometrics, the flow streamlines may be complicated curves while the concentration streamlines of the transferring species depend on only one distance coordinate. Such is the case, for example, for the rotating disk where the flow streamlines execute a spiral motion of increasing amplitude as the fluid moves toward the disk. The concentration, however, is a function only of axial location. In this instance, it is obviously desirable to avoid integrating along streamlines.

Consequently, the present analysis utilizes an Eulerian approach in which mass conservation of the vapor species and of each drop size is applied in a fixed control volume in the flow field. Drops in the unit volume may grow or evaporate, thereby depleting or augmenting the concentration of the monomer. The source term in the drop

conservation equations and the sink term in the monomer equation are derived from the microscopic balance equations of homogeneous nucleation kinetics. The effect of thermal radiation from the wall on the drop temperature is included by a heat balance on the drops. With this approach, the final results of classical infinite-medium nucleation kinetics are not directly used to modify the mass transfer problem. Rather, by integrating the nucleation rate equations into the drop conservation equations, an internally consistent description of the drop convection-diffusion-condensation process is obtained.

The equations were solved for the rotating disk flow geometry, which is one of the few fluid-mechanical systems which has an exact solution for the continuity, momentum, and energy equations.[15,16] This means that the velocities and temperature in the monomer and drop conservation equations can be determined from first principles; the correlations or approximations needed to solve other hydrodynamic systems are not required. The monomer and drop equations for the rotating disk also reduce to one-dimensional forms which simplifies the numerical solution. Experimental verification of the theory is also possible, since rotating disks can be operated as high as 2000°K. Experimental results will be reported in the second paper.

II. PROBLEM FORMULATION

Consider, first, the general conditions which produce nucleation and condensation in a boundary layer. Figure 1 shows a hot vaporizing surface surrounded by an inert gas. Two cases are shown: an isothermal case in which the gas is at the same temperature as the surface, and a non-isothermal case in which the gas far from the surface is considerably colder than the hot surface. In the isothermal case, the equilibrium vapor pressure is the same at all points in the boundary layer and is equal to the value at the wall. Since the partial pressure of the diffusing species decreases monotonically through the boundary layer from its value at the wall, it is always less than its equilibrium value and hence nucleation and condensation cannot occur.

In the non-isothermal case, the decrease in temperature through the boundary layer produces a rapid decrease in the local equilibrium vapor pressure. The equilibrium vapor pressure profile [$p_{eq}(T)$] may fall considerably below the isothermal diffusion-convection profile [$p^*(z)$] and hence nucleation and condensation can occur. In any event, the partial pressure of the monomer [$p(z)$] cannot fall below the local equilibrium profile; its exact location in this region, however, is determined by a mass balance between the drops of all sizes and the monomer.

A schematic of the vaporizing rotating disk is shown in Figure 2. The disk is infinite in extent and is surrounded

by a cold inert gas. Flow is assumed to be laminar. The surface of the disk is at constant temperature T_w while the gas far from the disk is at constant temperature T_∞. The disk rotates with angular velocity ω, which induces angular and radial velocity components in the gas in the boundary layer. Consequently the gas adjacent to the surface flows radially outward and by continuity the gas far above the surface flows downward. The molecules of the monatomically vaporizing substance diffuse out from the disk into the laminar boundary layer, the thickness of which can be shown to be independent of radius. If the conditions in the boundary layer are conducive to drop formation, monomer molecules may combine to form a droplet nucleus, or more probably, may combine with an existing drop by colliding with it.

The drops thus formed are convected with the bulk of the fluid (and also diffuse relative to the bulk flow) while growing or evaporating. The net motion of the drops relative to the bulk gas velocity was neglected in this analysis. This implies that the gravitational and centrifugal forces on the drops were negligible compared to the drag forces exerted by the bulk gas flow. This assumption is reasonable if very large drops are not formed.[17]

Only "dilute" systems were considered in this work.

While no precise concentration level separating "dilute" and "concentrated" mixtures is possible, the term dilute implies neglect of:

(1) Interfacial velocity.

(2) Property variations due to concentration changes in the boundary layer.

(3) The effect of heat release due to condensation on the boundary layer energy equation.

Most metal-inert gas systems, because of the low vapor pressure of the metal, are dilute; the methanol-air mixture considered by Epstein and Rosner[12] is not.

The effect of restrictions (1) - (3) above is to uncouple the momentum and energy equations from the material conservation equations. The momentum and energy equations, however, are still coupled to each other because of temperature induced physical property variations (viscosity, density, and thermal conductivity) in the boundary layer. The thermal-hydrodynamic problem, however, can be solved independently of the material conservation equations.

(1) The Conservation Equations

The equations describing steady-state mass, momentum, and energy conservation on a rotating disk are of the standard variety except for the temperature-induced variations in the transport coefficients. By appropriate variable transformations, these equations may be cast into

the constant property forms provided that the Prandtl number and the density-viscosity product can be assumed temperature independent.[17] Solution of this set of ordinary differential equations is straightforward and will not be detailed here. The necessary information which the hydrodynamic and energy equations provide is the gas temperature profile in the boundary layer and the axial velocity as a function of distance from the disk surface.

We confine attention here to the species conservation equations. It is a well known feature of rotating disk mass transfer that the concentration of the transferring species is a function only of axial distance from the disk. Anticipating that this independence of radial location holds in the presence of nucleation and condensation,[17] the equation governing conservation of monomer in the rotating disk boundary layer may be written as:

$$w \frac{df}{dz} = \frac{d}{dz}\left[\rho D \frac{d(f/\rho)}{dz}\right] + S_1 \qquad (1)$$

where w is the z-component of the hydrodynamic velocity, ρ is the density of the gas and D is the diffusion coefficient of the monomer in the inert carrier gas. The dependence of these quantities on axial position is provided by the solutions of the hydrodynamic and energy equations. f is the concentration of monomer in atoms/cm^3, which is related to its partial pressure by the ideal gas

law:

$$f = p/kT \tag{2}$$

S_1 is the monomer source term in atoms/cm^3-sec.

The conservation equation for drops containing g atoms is:

$$w \frac{dc_g}{dz} = \frac{d}{dz}\left[\rho D_g \frac{d(c_g/\rho)}{dz}\right] + S_g \tag{3}$$

where c_g is the concentration of size g drops in drops/cm^3, D_g is the diffusion coefficient for size g drops, and S_g is the source of size g drops in drops/cm^3. One such equation is required for each drop size g.

(2) The Droplet Source Term

The droplet source term S_g in Eq. (3) is obtained from the microscopic balance equations of nucleation kinetics.[3,4,6] Consider a distribution of drops of all sizes in a unit volume. Let A_g be the surface area of a drop of size g, β_g the rate at which vapor atoms in the gas condense upon a unit area of a drop of size g and α_g the rate at which atoms are evaporated from a drop of size g per unit area. Let J_g be the net rate at which drops pass from size g-1 to size g per cm^3 per sec, i.e., the droplet current in

g-space.* Since the product $\beta_{g-1}A_{g-1}c_{g-1}$ is the rate at which drops of size g-1 grow to size g per cm^3 per sec, and the product $\alpha_g A_g c_g$ is the rate at which drops of size g diminish to size g-1 per cm^3 per sec, the net rate J_g at which drops of size g-1 grow to size g is given by:

$$J_g = \beta_{g-1}A_{g-1}c_{g-1} - \alpha_g A_g c_g \tag{4}$$

The net rate S_g at which drops of size g are formed per cm^3 per sec is equal to the net rate at which drops of size g-1 grow to size g minus the net rate at which drops of size g grow to size g+1, i.e.

$$S_g = J_g - J_{g+1} \tag{5}$$

At this point, it is appropriate to review the various conditions under which drop current and drop source have been applied in other nucleation studies.

(1) The <u>balanced equilibrium</u> theory of homogeneous nucleation[2-6] applies to a system with no concentration

---

*The droplet current in g-space is very similar to the concept of the neutron slowing down density which occurs in calculations of the behavior of the neutron population in nuclear reactors.

gradients, no bulk flow, and no means of removing drops from the system. These conditions are summarized by the statements: $S_g = 0$, $J_g = 0$. Because balanced equilibrium theory requires abnormally high concentrations of drops larger than the "critical" size*, some means of removing growing drops must be included for nucleation theory to be applied to real systems.

(2) In the unbalanced equilibrium case[2-6] drops are permitted to grow through g-space at a constant rate; large drops are assumed removed from the system by an unspecified mechanism and returned to the vapor phase as monomer. Since this process is considered to be at steady state, and since no concentration gradients or bulk flow exist, it will be referred to as the infinite-medium steady-state case. It is characterized by the requirements: $S_g = 0$, J_g = constant. The source-free condition follows from Eq. (3) if the convective and diffusive terms are set equal to zero. The evaluation of the constant J for this case, which is commonly termed the nucleation rate, has been the subject of many studies.[2-7] Turkdogan[1] and Epstein and Rosner[12] have utilized the nucleation rate derived from the steady-state infinite-medium solution in their analysis of condensation effects on mass transfer in stagnant films.

(3) The infinite-medium transient case has been studied by various authors.[3,4,6,18,19] The governing

---

*The critical size drop is one that has an equal probability of growing or evaporating under the existing supersaturation.

equation in this case is $\partial c_g/\partial t = S_g = J_g - J_{g+1}$ which is the unsteady analog of Eq. (3) for an infinite medium.

(4) The present situation may be characterized as the finite-medium steady-state case because in the finite system, convection and diffusion of the monomer and drops must be considered.

(3) The Kinetic Coefficients

The condensation coefficient β_g is given by:

$$\beta_g = \eta_g \frac{p}{\sqrt{2\pi mkT}} \tag{6}$$

where m is the mass of a monomer atom and T is the local gas temperature. Eq. (6) assumes a sticking probability of unity and represents the Hertz-Knudsen equation modified by the factor η_g to give the correct transfer across the drop-vapor interface for large drops, i.e., drops whose growth rate is diffusion-limited rather than kinetically limited. The coefficient η_g is given by:[17,20]

$$\eta_g = \frac{1}{1 + (r_g/D)\sqrt{kT/2\pi m}} \tag{7}$$

For small drop radii r_g, η_g approaches unity and Eq. (6) reduces to the ordinary Hertz-Knudsen equation; for large drop radii Eqs. (6) and (7) reduce to the solution of the molecular diffusion equation for mass transfer from a sphere. Eq. (7) is not completely accurate for drop sizes on the order of the mean-free path; however, the contribution

of drops of this size or larger to the vaporization rate was found to be small and hence the error accured through this inaccuracy is very small.

The evaporation coefficient α_g is given by classical nucleation kinetics as:[3-5]

$$\alpha_g = \eta_g \left(\frac{A_{g-1}}{A_g} \right) \frac{p_{eq}(T_g)}{\sqrt{2\pi m k T_g}} \left(\exp \frac{2b}{3kT_g} g^{-1/3} \right) \tag{8}$$

where p_{eq} is the equilibrium vapor pressure and T_g the temperature of a drop of g atoms. The parameter b is:

$$b = 4\pi\gamma \left(\frac{3}{4\pi N} \right)^{2/3} \tag{9}$$

when γ is the surface tension of the bulk fluid and N is its density in atoms/cm^3. The area ratio A_{g-1}/A_g accounts for the fact that the surface area of a drop changes while adding or removing an atom, an effect which is important only for small drops. The relation between area and drop size is:

$$A_g = 4\pi \left(\frac{3}{4\pi N} \right)^{2/3} g^{2/3} \tag{10}$$

The exponential term in Eq. (8) accounts for the increase in the vapor pressure at the drop surface due to the finite radius of curvature of the drop. Note that α_g has been modified by a factor η_g to give the correct transfer rate for large drops.

There is still considerable controversy over the

proper form of the evaporation coefficient α_g.[21-24] In this work we used the classical form embodied in Eq. (8) because of the agreement between classical nucleation theory and experiment obtained by Katz and Ostermier.[7]

(4) The Boundary Conditions

Conservation of drops of size g atoms is described by Eq. (3) with the source term S_g given by Eqs. (4) and (5). It has been shown by Zeldovich[6] that S_g can be approximated by an expression involving the first and second partial derivatives of c_g with respect to g. This is accomplished by expanding S_g in a Taylor series in g and neglecting higher order terms. The result is an interesting situation in which the basic physics is expressed in finite difference form, whereas the differential form is an approximation. Since machine computation invariably requires approximation of partial derivatives by their finite difference analogs, nothing is gained by transforming the source term in the droplet conservation equations to derivative form.

However, the fact that the source term in Eq. (3) is equivalent to a second order partial derivative of the drop concentration c_g suggests that two boundary conditions on c_g in g-space are required. This is consistent with the fact that the infinite medium problem also requires two boundary conditions in g-space.[4-6] It is evident

that two boundary conditions are required in the z-direction because the problem is of the boundary layer type. These conditions are consistent with the mathematical form of Eq. (3) if S_g is represented by a second order partial derivative in c_g.[25] In this case Eq. (3) is an elliptic partial differential equation which requires two boundary conditions in both g and z; in addition, c_g must approach zero as g and z approach infinity.

In the z-direction, the boundary conditions are as follows. At the disk-vapor interface, the supersaturation is unity and the droplet concentration is assumed to be given by the balanced equilibrium model with unity supersaturation:[2-8]

$$c_g = f_w \exp\left(-\frac{b}{kT_w} g^{2/3}\right) \qquad \text{at } z=0 \text{ for all } g \qquad (11)$$

The subscript w denotes wall values (z=0) and f_w is $p_{eq}(T_w)/kT_w$. In the bulk gas far from the disk the droplet concentration must become vanishingly small, i.e.

$$c_g \to 0 \quad \text{as } z \to \infty \qquad \text{for all } g \qquad (12)$$

To determine the g-space boundary condition for the present problem, it is instructive to review the method of assigning the boundary conditions in the infinite-medium steady-state case. It is known that drops of small size spend most of their time oscillating back and forth

between larger and smaller g while only a few pass on to constitute the droplet current J.[4] So for small drops in the steady-state infinite-medium case, J of Eq. (4) is the small difference between two large numbers. Thus since $\beta_{g-1}A_{g-1}c_{g-1} >> J$ and $\alpha_g A_g c_g >> J$ then $\beta_{g-1}A_{g-1}c_{g-1} \simeq \alpha_g A_g c_g$ which leads to balanced equilibrium values of c_g. Hence, in the steady-state infinite-medium analysis, one boundary condition is that the solution must approach the balanced equilibrium solution as $g \to 1$.

In the present analysis, the balanced equilibrium boundary condition for small g could, in principle, be used provided that matching is done for a drop size smaller than the critical size. However, because the supersaturation can become very large at some points in the boundary layer, the critical drop size approaches unity. The kinetic coefficient α_g (Eq. (8)) is calculated from the bulk properties of the liquid, which is approximately correct for small drops but is clearly untenable for drops approaching atomic size. The normal technique in nucleation theory is to assume that the bulk properties of the liquid apply to drops greater than ten or twenty atoms in size.[3,18] Courtney,[18] who studied the infinite-medium transient case, matched his numerical solution to the balanced equilibrium solution at a drop size of twenty. Courtney's critical size was approximately sixty. Thus, if the critical drop size is sufficiently large, balanced equilibrium theory can provide a boundary condition without extensive

error in the calculation of the kinetic coefficient α_g. However, because the critical size in the present case was so small, this technique could not be used.

It became apparent during the calculations that a nucleation "zone" existed in the boundary layer; a zone formed approximately midway through the boundary layer where the nucleation rate was extremely high, and, in all other regions the nucleation rate was extremely low. Rosner and Epstein[12] also encountered this phenomenon of order of magnitude differences in nucleation rates. This produces the following result. Inside the nucleation zone, the concentration of small drops was determined primarily by nucleation kinetics, while outside the nucleation zone the concentration of small drops was primarily determined by diffusion and convection from the nucleation zone rather than by local nucleation. This type of behavior can result in numerical instabilities if one attempts to apply a nucleation kinetic boundary condition throughout the entire boundary layer, because the concentration of small drops outside the nucleation zone is not determined by nucleation kinetics alone but by diffusion and convection as well.

At the location of the maximum nucleation rate, the concentration of small drops (i.e. $g \leq g_o$, where g_o is an arbitrarily selected starting size) was assumed to be that given by the steady-state infinite-medium solution. This is a physically acceptable alternative to the balanced equilibrium boundary condition because the steady-state

infinite-medium solution is, in fact, the solution that does exist in an infinite medium as drops grow beyond the critical size. Using this solution is equivalent to assuming that the droplet currents J_g are large compared to the sum of the diffusive and convective terms in Eq. (3), i.e., that $J_g >> S_g$, $J_{g+1} >> S_g$, $S_g \approx 0$ at $g=g_o$. Thus by Eq. (5), $J_g \approx J_{g+1} \approx$ constant, which is the basis of the infinite medium solution.

Since the nucleation zone is a region of high supersaturation, the droplet growth rate is much greater than the droplet evaporation rate for drops larger than the critical size, and so from Eq. (4)

$$c_g \approx J/\beta_g A_g \quad , \qquad g \leq g_o \tag{13}$$

where J is given by the steady-state infinite-medium expression:[4,7]

$$J = \sqrt{\frac{2}{\pi}} \left(\frac{p_{eq}}{kT}\right)^2 \sqrt{\frac{\gamma}{m}} \; \frac{1}{N} \; S^2 \exp\left(\frac{-16\pi}{3} \cdot \frac{\gamma}{kT}^{\,3} \frac{1}{N^2} \; \frac{1}{(\ln(S))^2}\right) \tag{14}$$

where S is the supersaturation:

$$S = p/p_{eq} \tag{15}$$

For a specified variation of the temperature T and the monomer partial pressure p with position in the boundary

layer, the nucleation rate J(z) is determined by Eq. (14). At some location, z_{max}, J is a maximum. At this point, the concentration of drops of size g_o was assumed given by Eq. (13).

The concentration of drops of size g_o is also known at two other points in the boundary layer, namely at z=0 where c_{g_o} is given by Eq. (11) and $z=\infty$, where c_{g_o} is zero. An interpolation scheme is required to infer values of c_{g_o} at all other z from the known values at these three reference locations in the boundary layer.

To faithfully reflect the importance of transport processes in establishing the concentration of small drops outside the nucleation zone, interpolation was accomplished by determining $c_{g_o}(z)$ from the solution of the diffusion-convection equation, Eq. (3), with $g=g_o$. To effect this auxillary solution, the source term S_{g_o} was approximated by a constant times the local nucleation rate, J of Eq. (14). While this approximation to S_{g_o} has no theoretical justification, the precise description of the small-g source term is not important as long as it is small compared to diffusion-convection outside the nucleation zone.

In this manner, the concentration of drops of the selected starting value size was determined for all z. This auxillary solution furnished the small-g boundary condition for the full coupled set of conservation equations represented by Eqs. (1) and (3).

The boundary condition for large drops was

$$c_g \to 0 \text{ as } g \to \infty \qquad \text{for all } z \qquad (16)$$

The value of g_o was varied between 10 and 150 atoms; the results were found to be insensitive to the value used.

The concentration of monomer atoms at the wall f_w was taken as the equilibrium value. The net mass flux at the wall is small compared with the rate at which atoms leave the surface and condense upon it. The surface kinetic limitations characteristic of vacuum vaporization are absent since boundary layer diffusion is by far the slowest step in the overall process. Hence the equilibrium vapor pressure is obtained at the disk surface. At large z, $f \to 0$.

(5) The Monomer Source Term

The monomer source term S_1 in Eq. (1) is found as follows. Both sides of Eq. (3) are multiplied by g and the resulting equations summed for all $g \geq g_o$. When this sum is added to the monomer conservation Eq. (1), the result is a conservation statement for the vaporizing species in any form - drops or monomer. Since the source term in this total species balance must be zero, then

$$S_1 = -\sum_{g=g_o}^{\infty} gS_g \qquad (17)$$

The coupling between the monomer and droplet equations can now be clearly seen. The source term S_1 in the monomer balance depends upon the droplet source S_g by Eq. (17) and S_g depends upon the droplet concentration c_g via Eqs. (4) and (5). The coefficient β_g in Eq. (4) depends upon the monomer partial pressure p by Eq. (6), and p is related to the monomer concentration f via Eq. (2). Finally, f is determined by Eq. (1), which contains S_1.

(6) The Drop Temperature

Only the temperature T_g of a drop of size g atoms remains to be specified for a well-defined problem. Since the drop is in a strong thermal radiation field, it may not be at the temperature of the surrounding gas. A quasi-static energy balance upon the drop gives the following transcendental equation for T_g:[17]

$$\frac{1}{2}\sigma\varepsilon T_w^4 A_g + \ell(\beta_g - \alpha_g)A_g = \sigma\varepsilon T_g^4 A_g + C_p A_{th}\beta_{gas}(T_g - T)A_g \tag{18}$$

In this equation, σ is the Stephan-Boltzmann constant, ε the emissivity of the drop surface, and ℓ is the latent heat of vaporization. The heat capacity of the inert gas and the thermal accomodation coefficient of the inert gas atoms on the drop surface are denoted by C_p and A_{th} respectively. β_{gas} is the Hertz-Knudsen coefficient of the inert gas, given by Eq. (6) with the monomer partial

pressure replaced by the inert gas pressure and the mass m denoting the mass of the inert gas species. The first term in Eq. (18) represents the quantity of heat radiated from the disk to the drop, the second term represents the heat added to the drop by condensation of vapor on the drop, the third term is the heat radiated from the drop to the surroundings, and the last term is the quantity of heat removed from the drop by inert gas atoms colliding with the drop.

(7) The Solution Method

The advantage of the rotating disk as a vaporizing surface is that the governing equations can be reduced by a series of transformations to one-dimensional forms.[15,16] For the present case, the transformations of the conservation equations differ slightly from the usual rotating disk transformations because they include the effect of variable properties.[17] Inclusion of this effect was necessary because practical boundary layer nucleation experiments require very large temperature gradients.[1,9,17] Analytical solutions can then be obtained for the mass, momentum, and energy conservation equations if an approximate axial velocity profile is used.[17,26] However, analytical solutions cannot be obtained for monomer and droplet conservation equations because their source terms are complicated functions determined by nucleation kinetic relationships. Because of this, a computer program was written to solve the monomer

and droplet equations numerically.

If the drop conservation equation had to be solved for each drop size g, an enormous amount of machine time would have been required. Courtney[18] found that the amount of machine time became excessive if he attempted to carry his calculations beyond drop sizes of a few hundred atoms. To circumvent this difficulty, a multigroup scheme was formulated.* This consisted of combining a number of drop sizes into a single group. The droplet conservation Eq. (3) was then rewritten to describe the group-averaged drop concentration; the source term in this equation described the net transfer of drops across the ends of the group into adjacent groups. This multigroup scheme considerably reduced the amount of machine time required. The group-averaged equations are shown in Reference 17.

Two different estimates of the drop diffusion coefficient were investigated. In the first case, the diffusion coefficient of the drops was assumed to be equal to the diffusion coefficient of the monomer. The approximation $D_g = D$ makes the set of drop conservation Eqs. (3) much more tractable because the diffusion boundary layer thickness is the same for all drop sizes. The disadvantage of this approach is that it overestimates the mobility of the large drops.

In the second case, the diffusion coefficient of the drops was assumed to vary as the monomer diffusion

---

*Multigroup methods (in energy space) are common in nuclear reactor calculations.

coefficient divided by drop size to the two-thirds power.* The relation $D_g = D/g^{2/3}$ produces a variation in the diffusion boundary layer thickness[27] of a factor of twenty for drop sizes covering a range of 10^6 atoms. This large variation in the boundary layer distance between equations in a coupled set requries a novel approach in order to obtain accurate numerical solutions. To avoid the computational problems which would have resulted if some of the equations had to be solved numerically over a distance many times their boundary layer thickness, the method of singular perturbation was used.[28] For each drop size, the procedure consisted of developing an inner expansion within the droplet boundary layer and an outer expansion beyond it and then matching the two solutions in a suitable fashion to give a continuous solution. The application of this technique is discussed in more detail in Reference 17.

The division of the boundary layer into inner and outer regions is not simply a mathematical artifice but reflects the following physical situation. In the inner

---

*This is the classical molecular diffusion relationship and is strictly true for drops smaller than the mean-free path.[20] Since it will be shown that there are few drops larger than the mean-free path in the iron-argon rotating disk system, this approximation can safely be used for all drop sizes.

region, the concentration is determined by a balance between diffusion and convection, and the source term is of second order. In the outer region, the concentration is determined by a balance between the convective term and the source term and diffusion is of second order. This is what would be expected physically; applying the method of singular perturbation makes it clear mathematically.

The droplet conservation equation was solved for a discrete set of groups covering a range of approximately 10 to 10^{20} atoms. A range in g of this magnitude was required even though drops of size greater than 10^9 atoms made no contribution to the monomer source term and thus had no effect upon the vaporization rate or the coupling between monomer and droplet equations. The boundary condition for large g required setting the drop concentration equal to zero at some large size; unless this point was considerably beyond 10^9 atoms, an influence upon the droplet concentration at sizes less than 10^9 atoms, and hence an influence upon the vaporization rate, was found.

The calculations were made for disk temperatures ranging from 1500°K to 1900°K; the iron disk was assumed to be vaporizing in argon with an ambient temperature of 300°K. The properties of iron which were used in the nucleation kinetic relationships, such as surface tension and vapor pressure and density, were obtained from Refs. 1, 29, and 30.

III. ENHANCEMENT OF THE VAPORIZATION RATE

The change in the vaporization rate in a system with condensation enhancement from that in an isothermal system is due to three factors:

(1) Condensation

(2) Property variations

(3) Thermal diffusion (the Soret effect)

All three of these effects are due to the extremely large temperature difference (up to 1500°C) across a boundary layer which is only a fraction of a centimeter thick.

The fractional increase in the vaporization rate due to temperature-induced property variations can be shown to be:[17]

$$[(\rho^2 D)_w/(\rho^2 D)_\infty]^{1/2}$$

where the subscript ∞ denotes bulk conditions. If $D \sim T^2$ and $\rho \sim 1/T$, property variations do not affect the vaporization rate. For the iron-argon system, $D \sim T^{1.95}$, and so this condition is approximately true.[17] Because of this, property variations will be neglected.

The effect of thermal diffusion can be evaluated independently of the first two; an analysis of its effect shows it to be small for the iron-argon system at temperatures below the melting point of iron.[17]

The mass flux at the wall is the sum of the fluxes due to monomer and drop of all sizes:

$$j_w = j_1 + \sum_{g=g_o}^{\infty} j_g \tag{19}$$

or:

$$j_w = -m(\rho D)_w \left[\frac{d}{dz} \left(\frac{f}{\rho}\right) + \sum_{g=g_o}^{\infty} g\left(\frac{D_g}{D}\right) \frac{d}{dz} \left(\frac{c_g}{\rho}\right) \right]_w \tag{20}$$

If the system could be considered source-free and the fluid properties are constant, then Eq. (1) has an analytic solution if the dimensionless axial velocity profile is approximated by a straight line.[26] Applying this approximation to an isothermal rotating disk then gives the mass flux at the wall as:

$$j_w^* = m f_w D_w \sqrt{\frac{\omega}{\nu_w}} \sqrt{\frac{Sc_w}{2\pi}} \tag{21}$$

where ν is the kinematic viscosity of the fluid, and Sc the Schmidt number (ν/D). Since it is immaterial where one evaluates the properties in an isothermal system, we have arbitrarily evaluated them at the wall (denoted by subscript w).

Since the isothermal, source-free mass transfer rate in a rotating disk system is well known, the effects due to non-isothermal conditions are best presented by computing the ratio of the mass fluxes in the two cases:

$$j_w/j_w^* = \phi \tag{22}$$

ϕ is the factor by which the isothermal transfer rate is enhanced by condensation.

The enhancement due to condensation can be calculated by three methods:

(1) Bulk equilibrium condensation

(2) Critical supersaturation using the Turkdogan-Rosner method

(3) Present theory.

In case (1), condensation is not kinetically limited and the equilibrium vapor pressure is assumed to be attained at each point in the boundary layer. The monomer concentration gradient at the wall is obtained directly from the gas temperature profile and the equilibrium vapor pressure-temperature relationship, and drop diffusion and convection need not be considered. Assuming a linear axial velocity profile,[26] and solving the rotating disk energy equation in conjunction with the Clauius-Clapeyron equation yields for this model:[17]

$$\phi = \left(\frac{Pr}{Sc}\right)^{\frac{1}{2}} \frac{\ell}{kT_w} (1 - T_\infty/T_w) \tag{23}$$

where ℓ is the latent heat of vaporization, k is the Boltzmann constant, and Pr the Prandtl number. This derivation neglects the effect of heat release due to condensation. Hills and Szekeley[31,32] and Rosner and Epstein[12] have derived analogous formulae for ϕ which include the heat release due to condensation but are

restricted to systems with a Lewis number (Sc/Pr) of unity. Their results show that the effect of latent heat release is less than 4% for the cases considered here, i.e., for iron-argon systems below the melting point of iron. For this reason the effect of release of latent heat in the boundary layer has been neglected in the present analysis.

The results of the critical supersaturation model, case (2), can also be expressed by a condensation factor. This was done using Turkdogan's[1] graphical method and Eq. (14). Rosner's analysis,[10] although more convenient, could not be used because it requires that the logarithm of the critical supersaturation be a linear function of reciprocal temperature; at temperatures which are practically attainable with a rotating disk in an iron-argon system, this is definitely not true. In calculating ϕ, a nucleation current J of 10^{12} was used. This corresponds to the value which Epstein and Rosner[12] found in their boundary layer study. The properties in the nucleation equation (Eq. (14)), such as surface tension and density, were evaluated at the film temperature of the boundary layer.

The effect of nucleation in the boundary layer on the vaporization rate from a rotating disk is shown in Figure 3. Here the condensation factor ϕ is shown as a

function of the disk temperature T_w for a rotational speed of 1500 rad/sec. The effect of drops diffusing back into the wall, (i.e., the sum in Eq. (20)) was neglected because it was less than 1% of the monomer mass flux at the wall in all cases. In the case of no condensation, ϕ is independent of temperature and has a value of unity. Below 1600°K, Figure 3 indicates that the effect of condensation is nil; above 1600°K, the effect increases rapidly with temperature. At 1900°K, the enhancement is a factor of two and one-half for the case $D_g = D$, and a factor of six for the case $D_g = D/g^{2/3}$.

The greater enhancement in the variable diffusivity case is caused by the fact that the lower diffusivity of the larger drops in this case gives them less mobility, which has two consequences.

First, the large drops find it more difficult to diffuse into the region close to the wall there the convective transport is weak. The region close to the wall is much hotter than the outer regions and a drop which tended to grow in the cooler outer region tends to evaporate, or at least grow much less rapidly, near the wall. The drops tend to evaporate in this region because the evaporation coefficient α_g is a very sensitive function of temperature and increases rapidly as the temperature is increased. Thus the ability of the drops to evaporate is smaller in the variable diffusivity case and so the monomer sink is larger and hence the wall gradient is increased.

The second effect arises from drops leaving the nucleation zone in the direction of the outer boundary layer edge. As the diffusion coefficient becomes smaller, the ability of the drops to move outward against the convective inflow is impaired. Thus low diffusivity drops have a greater tendency to stay in that part of the boundary layer where their capacity to absorb monomer is larger. Thus the smaller drop diffusion coefficient of the variable diffusivity case effectively stops the large drops in the region of the boundary layer where they can most efficiently remove monomer from the vapor phase.

It can be seen in Figure 3 that the two effects described above increase the condensation factor in the variable diffusivity case over that of the constant diffusivity case by significant amounts at high temperature. However, the point at which nucleation becomes significant (1600°K) is practically the same in the two cases. This is consistent because a variation in the drop diffusion coefficient cannot affect the wall gradient until a large number of drops are formed by nucleation.

The Turkdogan-Rosner results are also shown in Figure 3. The enhancement in this case in approximately equal to that of the constant diffusivity case. The results of the bulk equilibrium condensation model are not shown, but give values of ϕ ranging from 20.4 at 1500°K to 16.0 at 2000°K.

IV. STRUCTURE OF THE NUCLEATION ZONE IN THE BOUNDARY LAYER

Figure 4 shows a profile of a typical nucleation rate J as a function of axial distance through the boundary layer. The axial distance is expressed in terms of a dimensionless distance x which is related to z by:

$$x = \left[\frac{(\rho\mu)_\infty}{(\rho\mu)_f}\right]^{1/2} \left(\frac{\omega}{\nu_\infty}\right)^{1/2} \int_0^z \left(\frac{\rho}{\rho_\infty}\right) dz' \tag{24}$$

where the subscripts ∞ and f denote bulk gas and film average conditions respectively. If property variations are neglected, Eq. (24) reduces to the standard distance variable transformation for the rotating disk.[15] The value of J was calculated from the classical Becker-Döring-Zeldovich expression, Eq. (14), using the monomer partial pressure profile which was a solution of Eqs. (1) and (3). The important characteristic of the figure is the existence of a "nucleation zone", i.e., a region where the nucleation rate is very high, and which is surrounded on either side by regions with relatively low nucleation rates. It is in this nucleation zone that the drops are formed. Such a zone was also found by Epstein and Rosner.[12] The maximum nucleation rate in the zone occurs at $x \approx 2\ 1/4$, or between one-half and three-quarters through the boundary layer; the rotating disk flow boundary layer is generally considered to end at $x \approx 3\ 1/4$.[15] In addition to being skewed toward the outer region of the boundary layer, the zone

(if measured by its width at half-maximum) occupies approximately 50% of the boundary layer. The nucleation rate in the first third of the boundary layer ($0 < x < 1$) is essentially zero compared to the rate further out in the boundary layer. The nucleation rate in the nucleation zone is approximately 10^{14} drops/cm^3-sec, which is comparable to the maximum rate of 10^{14} drops/cm^3-sec in Epstein and Rosner's study.[12] No special significance should be attached to this accord however, for it is not obvious why nucleation rates should be the same in different systems.

Figure 5 shows a typical drop size distribution in the nucleation zone ($x = 2\ 1/4$) and also near the wall ($x = 1/4$). The infinite-medium steady-state solutions are also plotted for comparison.

In the nucleation zone ($x = 2\ 1/4$) the boundary layer solution approaches the infinite-medium solution for $g \leq g_o$, as is required by the boundary condition. For large drops, it falls increasingly below the infinite-medium solution as drop size increases. This is the expected behavior because in the infinite-medium solution the droplet current J is a constant and hence the same number of drops pass through each size. In the boundary layer case, drops can also leave an incremental volume element by convection and diffusion; since the transport by these mechanisms in the nucleation zone results primarily in an outflow of drops to other regions, the

boundary-layer concentration should lie below the infinite-medium concentration.

Near the wall (x = 1/4), however, few drops are formed and the transport mechanisms in general produce an inflow of drops into this region. Hence the boundary layer concentration should be larger than the infinite medium concentration, and Figure 5 indicates that this is in fact so.

The balanced equilibrium solution at x = 2 1/4 is also shown in Figure 5. The minimum of the balanced equilibrium curve occurs at the critical drop size and the figure indicates that this is approaching atomic size. The value of g_o, i.e., the matching point between the infinite-medium and boundary layer solutions, was ten in this case and is shown in the figure.

Figure 6 shows the variation of the dimensionless droplet evaporation and condensation coefficients with axial position in the boundary layer for a typical drop size. The evaporation coefficient α_g is higher than the condensation coefficient β_g in the vicinity of the wall where the temperature is high. This is because the vapor pressure is a rapidly increasing function of temperature and the evaporation coefficient is proportional to the vapor pressure at the drop temperature. As the temperature decreases with increasing axial distance through the boundary layer, the evaporation coefficient decreases rapidly and in fact is considerably smaller than the

condensation coefficient throughout most of the boundary layer. The linear scale is somewhat deceptive at large distances for at $x \approx 4$, the evaporation coefficient is orders of magnitude less than the condensation coefficient. However, the important point is that drops very close to the wall tend to evaporate rather than grow.

Figure 7 shows the monomer source term as a function of axial distance through the boundary layer for a typical case. The source is positive close to the wall because the droplet evaporation coefficient is larger than the droplet condensation coefficient there. The source, however, rapidly becomes negative at an axial distance $x = 1/4$ because the evaporation coefficient decreases much more rapidly than the condensation coefficient. Thus, drops formed in the nucleation zone and transported toward the wall grow very rapidly in this region, and in doing so consume monomer, thus driving the monomer source term to large negative values. Note that Figure 4 indicates that very few drops are nucleated in the region where the large negative source term occurs ($x \approx 1/4$) and Figure 7 indicates that little monomer is consumed in the nucleation zone ($x \approx 2\ 1/4$). The small drops born in the nucleation zone consume relatively little monomer while being transported out of it; however, as they grow into large drops nearer the wall, the amount of monomer they consume increases tremendously. This is consistent with the results of steady-state infinite-

medium theory where it has been found that the larger drops consume the most monomer.[4] As the axial distance from the wall increases farther, the monomer source term becomes small because the monomer concentration, and hence the droplet condensation coefficient, has been depressed to the point where the drops grow much more slowly. Thus the monomer depletion rate becomes small.

The oscillatory nature of the monomer source (Figure 7) causes many numerical problems. It was the principal reason that the calculation could not be made for very large enhancements in the vaporization rate, (i.e., for vaporization rates approaching the bulk equilibrium condensation rate value) or for nucleation models such as that of Lothe and Pound,[24] which give much larger nucleation rates than the classical theory under the same conditions. The reason for this is that the monomer source is, in effect, the small difference between two very large numbers and any error made in computing the source in the positive or negative source regions of Figure 7 has a large effect on the monomer concentration.

Figure 8 shows the dimensionless contribution from the individual groups to the monomer source term for a typical case. The profile in g-space was taken at the position of the maximum monomer sink, $x \approx 1/4$. Plotted on the ordinate is the product $g \cdot S_g(x)$, which is the contribution to the monomer source from drops of size g. The total monomer source is given by the negative of

the sum of the contributions from the individual groups (Eq. (17)), and so is approximated by the area under the curve in Figure 8. The figure shows that drop sizes between 10^3 and 10^6 are the principle contributors to the monomer source; drop sizes below 10^3 and above 10^6 make negligible contributions. Small drops contribute little to the monomer sink because their small surface area does allow them to consume significant quantities of vapor. For drop sizes greater than 10^6, the contribution to the monomer source term approaches zero because the drop concentration becomes so small (see Figure 5). Thus only intermediate drop sizes contribute to the source term.

Figure 9 shows the ratio of the drop temperature to the wall temperature as a function of drop size for a particular location in the boundary layer as given by the energy balance Eq. (18). For most of the drop sizes shown, the drop temperature is equal to the temperature of the surrounding gas; only at large drop sizes does the drop temperature differ from the gas temperature. As the drop increases beyond 10^{15} atoms in size, the drop temperature rises quite rapidly because of heat transferred by thermal radiation from the wall to the drop, and it approaches the wall temperature at sizes approaching 10^{20}. The reason that the drop temperature remains very close to the gas temperature over such a large range is that the rate at which heat is removed from the drop by gas

atoms colliding with it is very large. That is, the coefficient of the fourth term in Eq. (18), is large. The coefficient β_{gas} is directly proportional to the pressure of the surrounding gas. In the calculations presented here, the inert gas pressure was assumed to be one atmosphere. For nucleation in rarified environments, however, the effect of radiation would become very important because the heat removed by the inert gas atoms colliding with the drops would be much smaller. Hence, the drop temperature would depart from the gas temperature at much smaller drop sizes. At any total pressure, the population of large drops would be limited by radiation heating.

V. EFFECT OF SOME PARAMETRIC VARIATIONS

The effect of variations in the angular velocity of the rotating disk on the vaporization rate is shown in Figure 10, where the vaporization rate is plotted against the square root of the angular velocity. As expected from Eqs. (21) and (23), the vaporization rate in the bulk equilibrium condensation case and in the condensation-free case are directly proportional to the square root of the angular velocity. The vaporization rate in the nucleation kinetic case is not proportional to the square root of the angular velocity, as can be seen from the middle line of Figure 10. This difference in behavior is produced by the fact that the angular velocity controls the convection term in the conservation equations and

and hence the balance among diffusion, convection, and condensation is affected by disk speed.

Figure 11 shows surface tension decreases the vaporization rate, with all other parameters held constant. This is because the evaporation coefficient α_g decreases with decreasing surface tension and thus the rate at which drops evaporate is reduced, thereby increasing the monomer gradient at the wall.

VI. CONCLUSIONS

The structure of the nucleation zone in the gas film on a rotating disk is such that drops are produced in significant quantities only near the middle of the boundary layer. As shown in Figure 12, drops formed there are then transported by diffusion and convection into a region closer to the wall where rapid growth is favored. Finally, they move very close to the wall where they evaporate. This effect produces a cycle because the monomer produced by the drops evaporating is transported away from the wall and into the nucleation zone where some of it is reformed into drops which are again returned towards the hot surface. Thus a recycle is superimposed upon the ordinary outward transport of the vaporizing species which normally occurs in the isothermal boundary layer. Under the proper conditions, it is possible that the recycle mechanism could retard rather than enhance the vaporization rate. However, only rate enhancements were found for the range of input parameters studied here.

ACKNOWLEDGMENT

This work was performed under the auspices of the United States Atomic Energy Commission.

REFERENCES

(1) Turkdogan, E.T., Trans. AIME, 230, 740 (1964).

(2) Becker, R. and W. Döring, Ann. Phys. 24, 719 (1935); or NASA Tech. Memo. 1374.

(3) Frenkel, J., Kinetic Theory of Liquids, Clarendon Press, Oxford, Ch. 7, (1946).

(4) Farley, F.M.J., Proc. Roy. Soc., A, 212, 530 (1952).

(5) Barnard, A.J., Proc. Roy. Soc., A, 220, 132 (1953).

(6) Zeldovich, J.B., Acta Physicochimica, U.S.S.R., 18, 1 (1943).

(7) Katz, J.L., and B.J. Ostermier, J. Chem. Phys., 47, 478 (1967).

(8) Nucleation Phenomena, American Chemical Society Publication, Washington, D.C., (1966).

(9) Turkdogan, E.T. and K.C. Mills, Trans. AIME, 230, 750 (1964).

(10) Rosner, D.E., Int. J. Heat and Mass Transfer, 10, 1267 (1967).

(11) Elenbaas, W., Phillips Research Reports, 22, 1 (1967).

(12) Epstein, M., and D. Rosner, Int. J. Heat and Mass Trans.

(13) Wegener, P.P., and A.A. Pouring, Phys. of Fluids, 7, 352 (1964).

(14) Wegener, P.P., and L.M. Mack, Adv. Appl. Mech., 5, 307 (1958).

(15) Schlichting, H., Boundary Layer Theory, McGraw-Hill Book Co., p. 85 (1960).

(16) Dorfman, L.A., Hydrodynamic Resistance and the Heat Loss of Rotating Solids, Oliver and Boyd, London, England (1963) (translation from Russian).

(17) Omberg, R.P., UCRL-18577, (1969).

(18) Courtney, W.G., J. Chem. Phys,, 36, 2009 (1962).

(19) Kantrowitz, A., J. Chem. Phys., 19, 1097 (1951).

(20) Friedlander, S.K., J. Colloid, Interfac. Sci., 23, 157 (1967).

(21) Feder, J., J.C. Russell, J. Lothe, and G.M. Pound, Adv. Phys., 15, 111 (1966).

(22) Lothe, J., and G.M. Pound, J. Chem. Phys., 36 2080 (1962).

(23) Reiss, H. and J.L. Katz, J. Chem. Phys., 46 2496 (1967).

(24) Lothe, J. and G.M. Pound, J. Chem. Phys., 48, 1849 (1968).

(25) Tikhonov, A.N., and A.A. Samarskii, Equations of Mathematical Physics, Pergamon Press (1963) (translated from Russian).

(26) Olander, D.R., Ind. and Eng. Chem. Fund., 6, 178 (1967).

(27) Sparrow, E.M., and J.L. Gregg, J. Heat Transfer, 810, 249 (1959).

(28) Ames, W.F., Non-Linear Ordinary Differential Equations in Transport Processes, Academic Press (1968).

(29) Grosse, A.V., J. Inorg, and Nucl. Chem., 26, 1349 (1964), and Science, 140, 791 (1963).

(30) Nesmeyamov, A.N., Vapor Pressure of the Elements, Elsevier Publishing Co., New YOrk (1963).

(31) Hills, A.D.W., and J. Szekely, Chem. Eng. Sci., 19, 79 (1964).

(32) Hills, A.D.W., and J. Szekely, Int. J. Heat and Mass Transfer, 12, 111 (1969).

FIGURE CAPTIONS

(1) Schematic of temperature and partial pressure profiles during isothermal and non-isothermal vaporization

(2) Rotating disk geometry

(3) Enhancement of the rate of vaporization of iron into argon

(4) Variation of the nucleation rate through the boundary layer

(5) Drop concentrations at two positions in the boundary layer

(6) Variation of evaporation and condensation coefficients through the boundary layer

(7) The monomer source in the boundary layer

(8) Contribution to the monomer source from drops of different sizes at $x = 1/4$

(9) Ratio of drop temperature to wall temperature in the nucleation zone

(10) Effect of disk rotational speed on the vaporization rate

(11) Effect of drop surface tension on the vaporization rate

(12) Schematic of vapor recycle in the non-isothermal boundary layer of a rotating disk

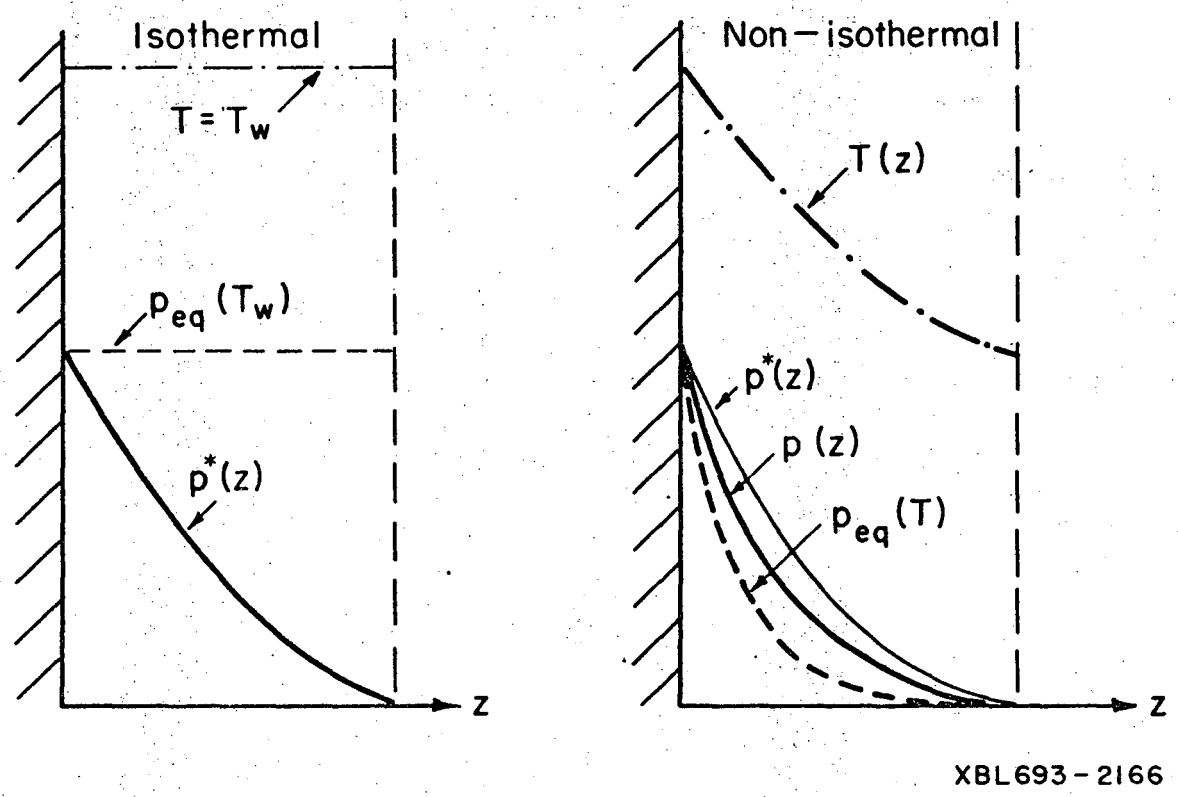
Isothermal
T = Tw
peq (Tw)
p*(z)
z
Non-isothermal
T (z)
p*(z)
p (z)
peq (T)
z
XBL693-2166

Fig. 1

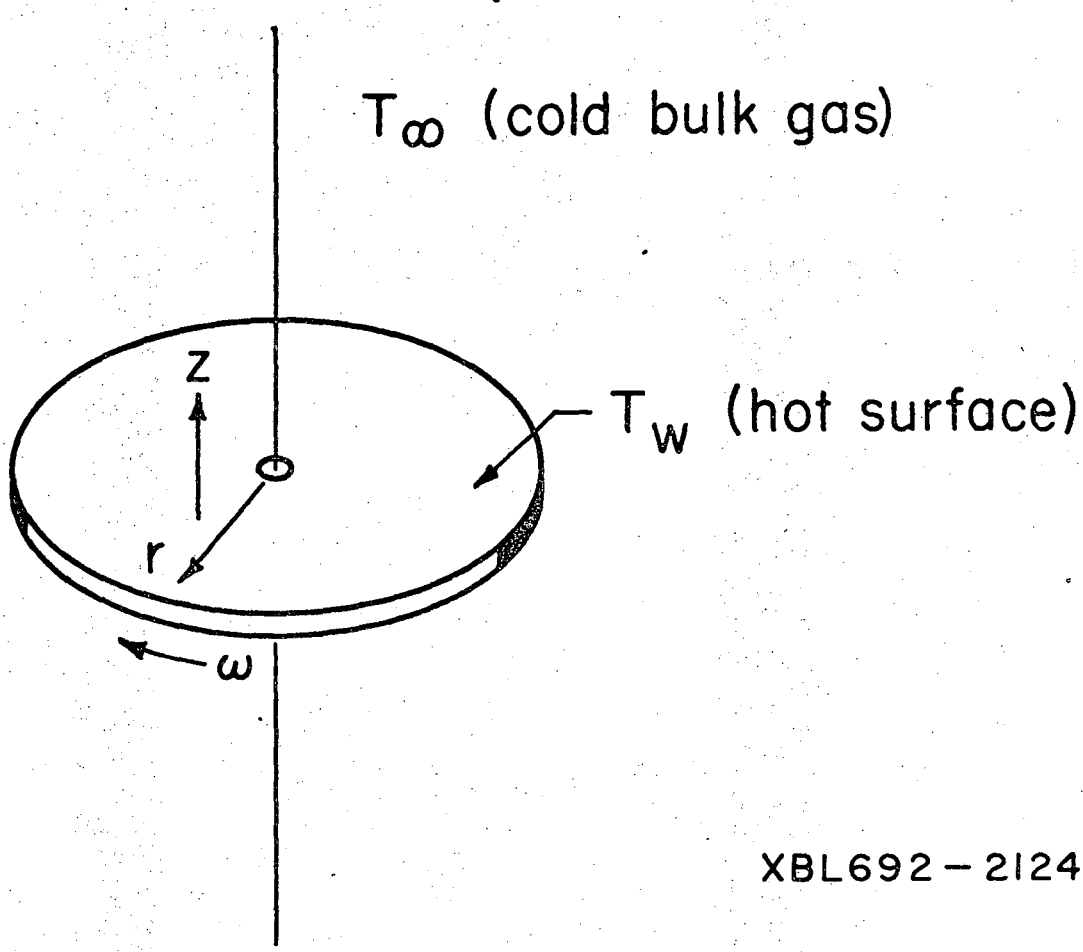

Fig. 2

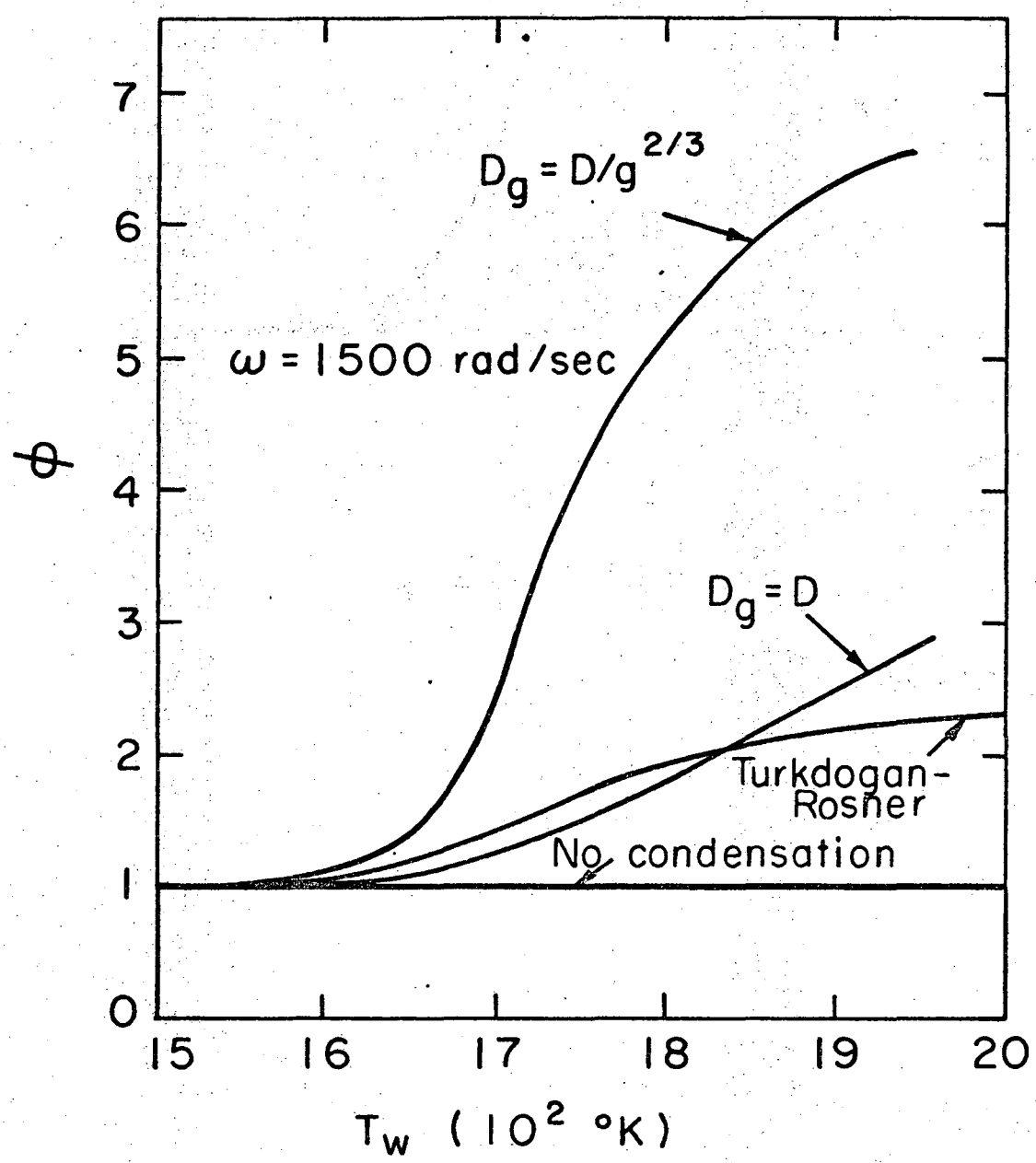

XBL705-2876

Fig. 3

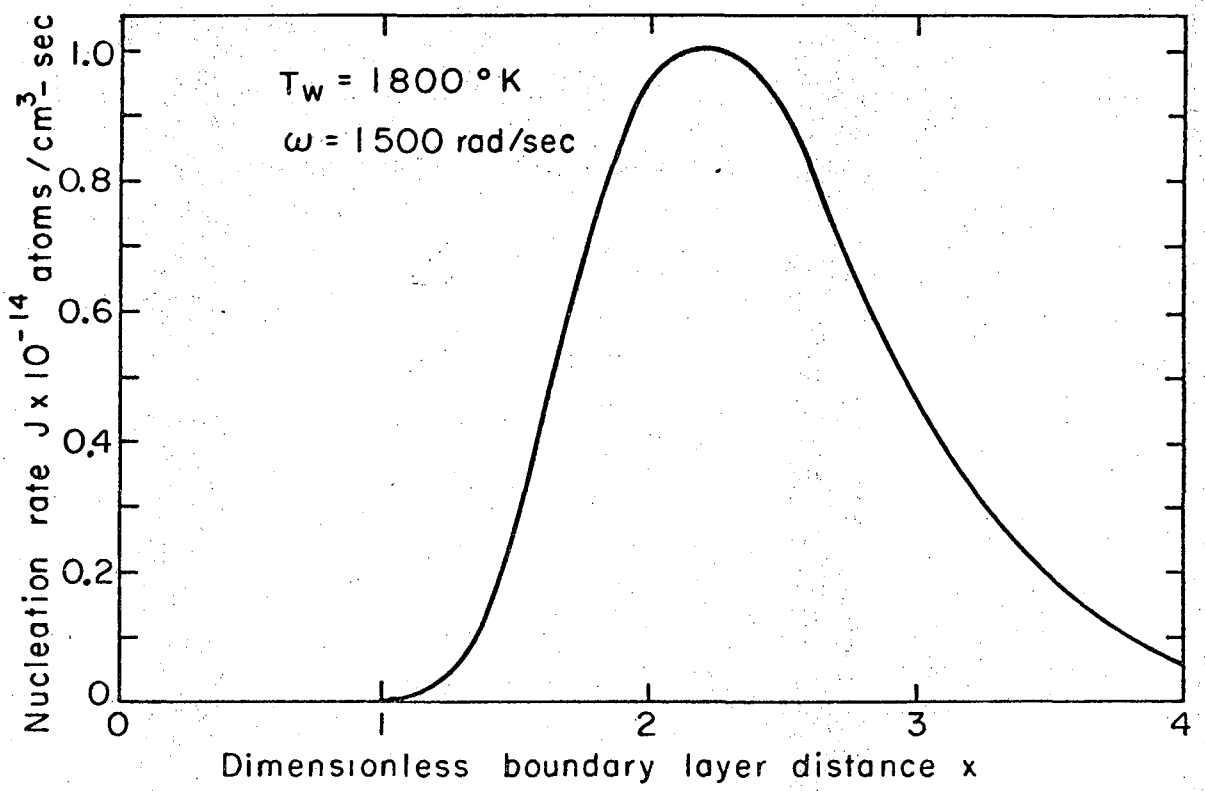

XBL705-2877

Fig. 4

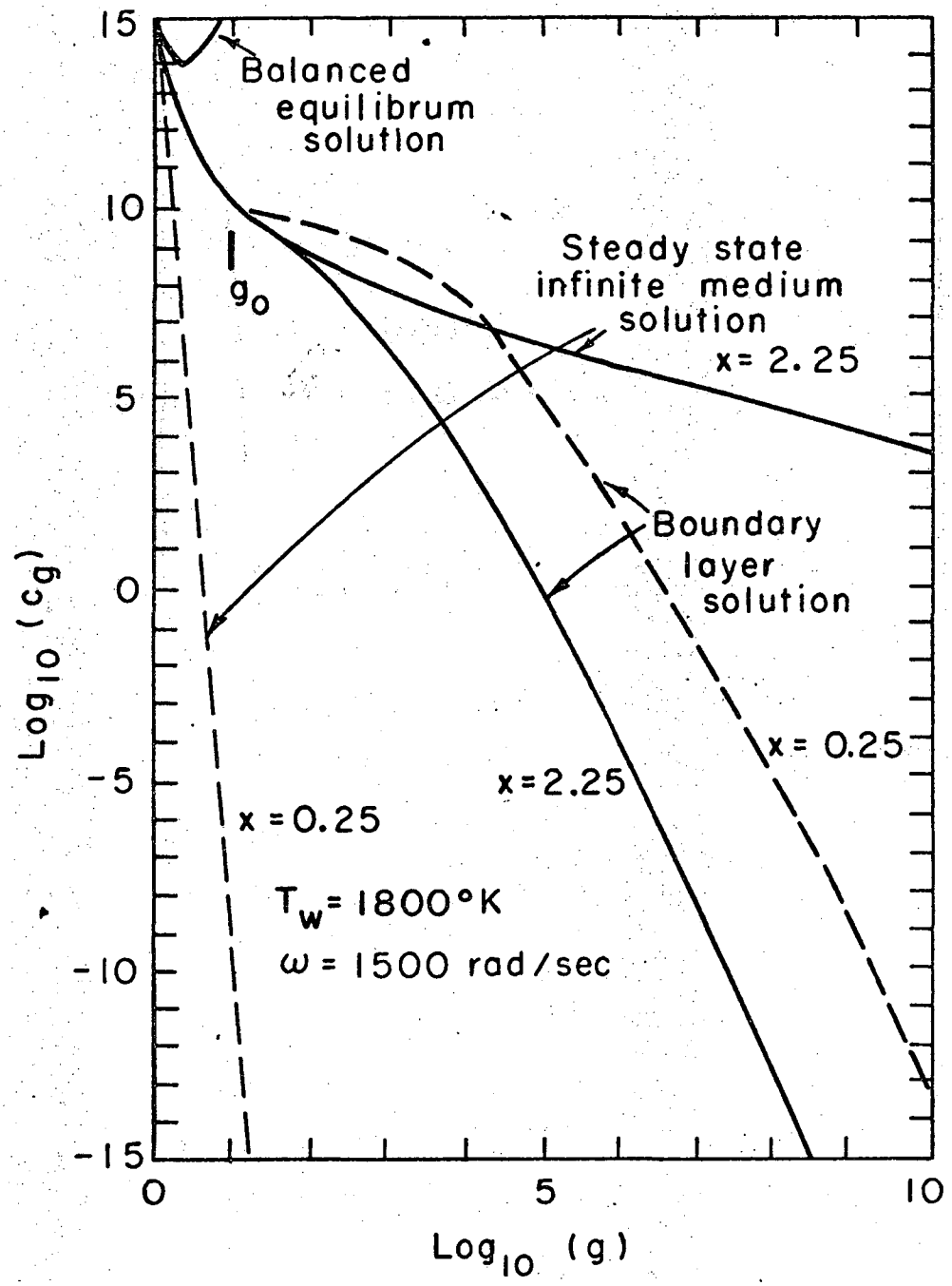

XBL705-2878

Fig. 5

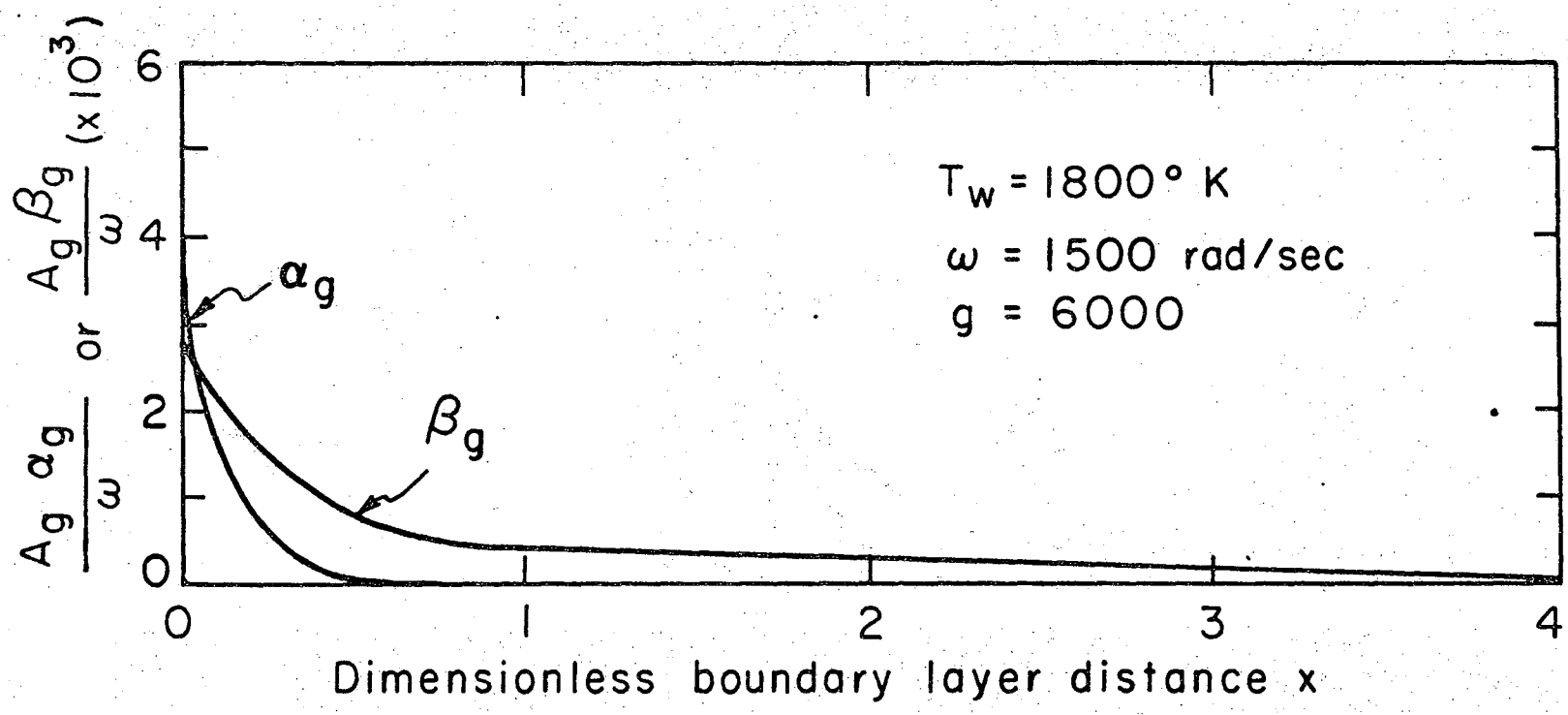

XBL705-2879

Fig. 6

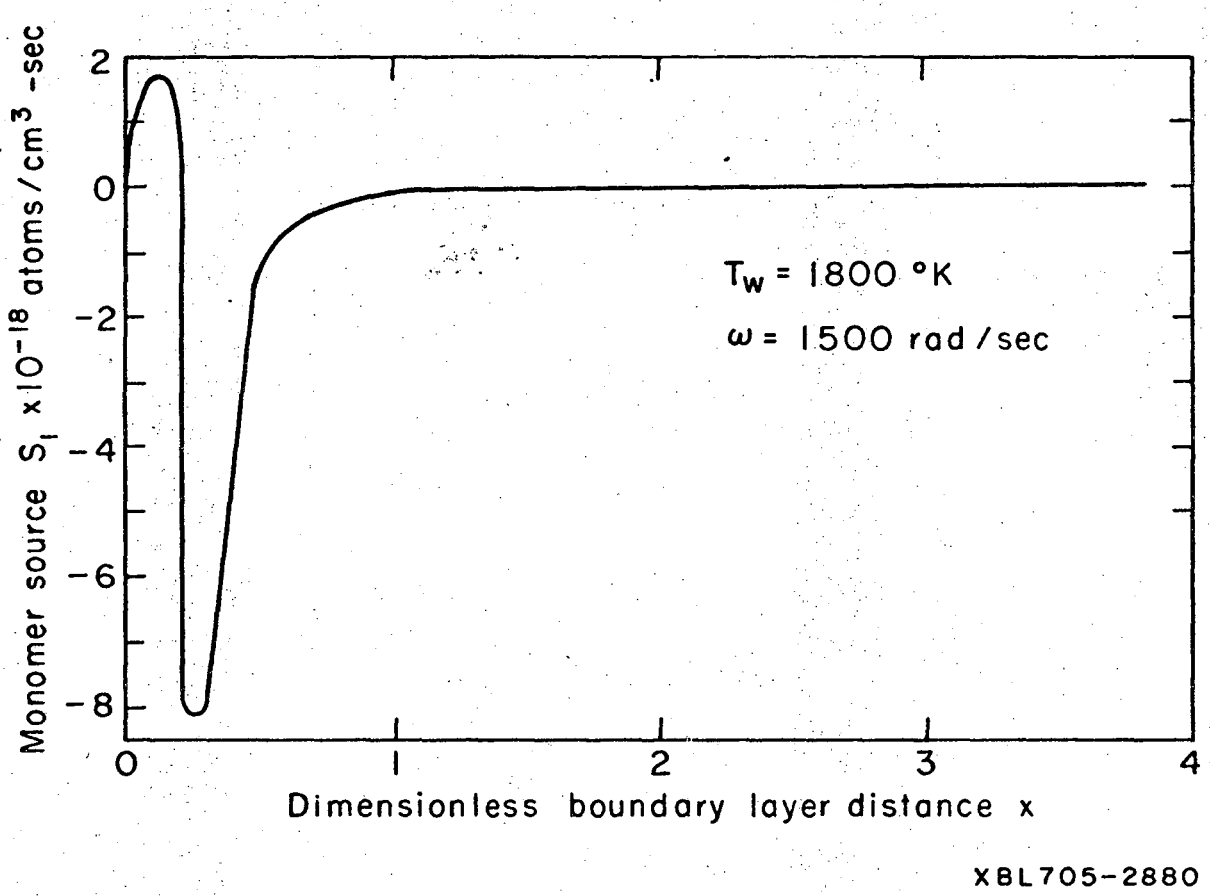
Monomer source $S_1 \times 10^{-18}$ atoms/cm^3-sec
2
0
-2
-4
-6
-8
0
1
2
3
4
Dimensionless boundary layer distance x
T_w = 1800 °K
ω = 1500 rad/sec
XBL705-2880

Fig. 7

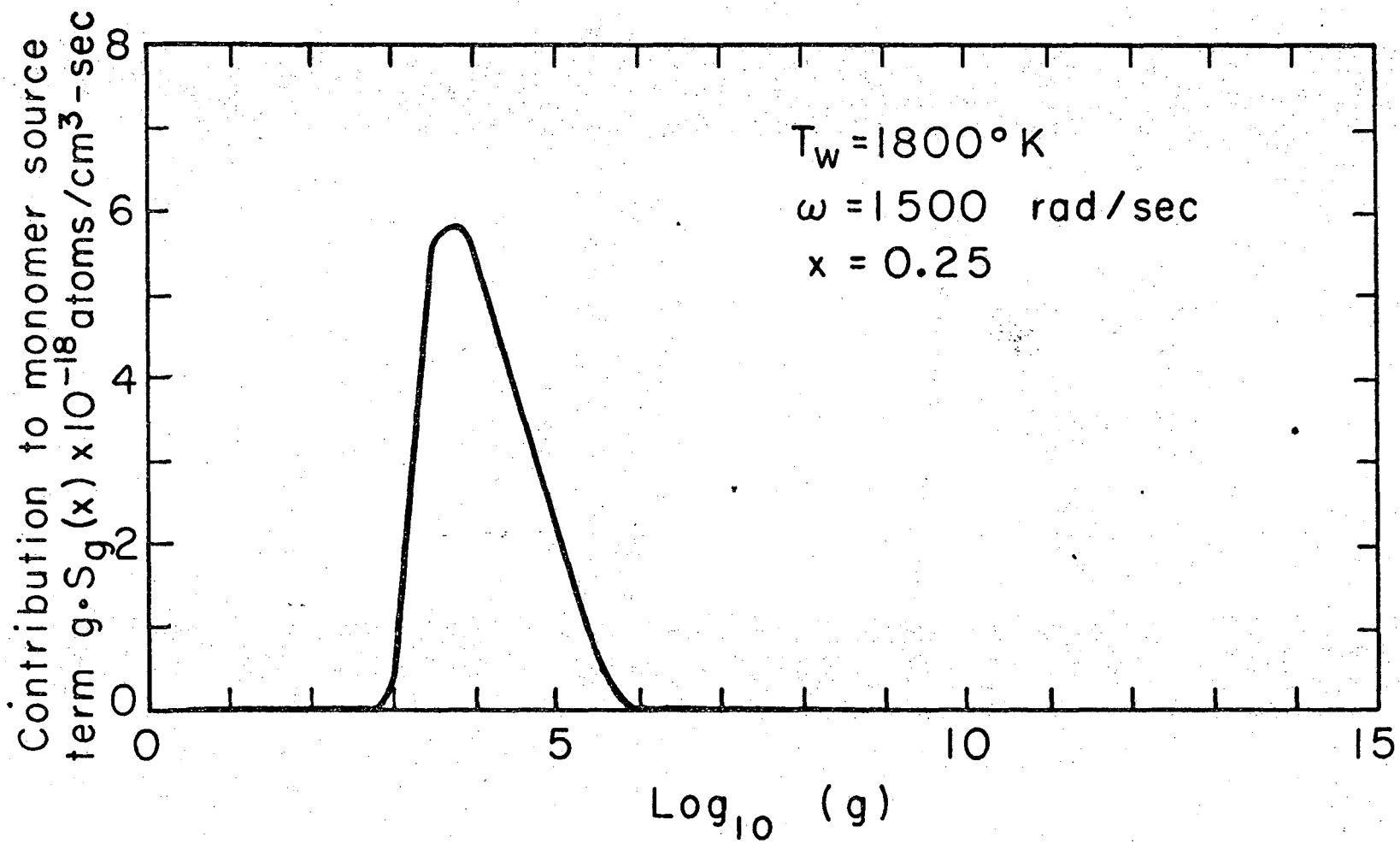

XBL705 - 2881

Fig. 8

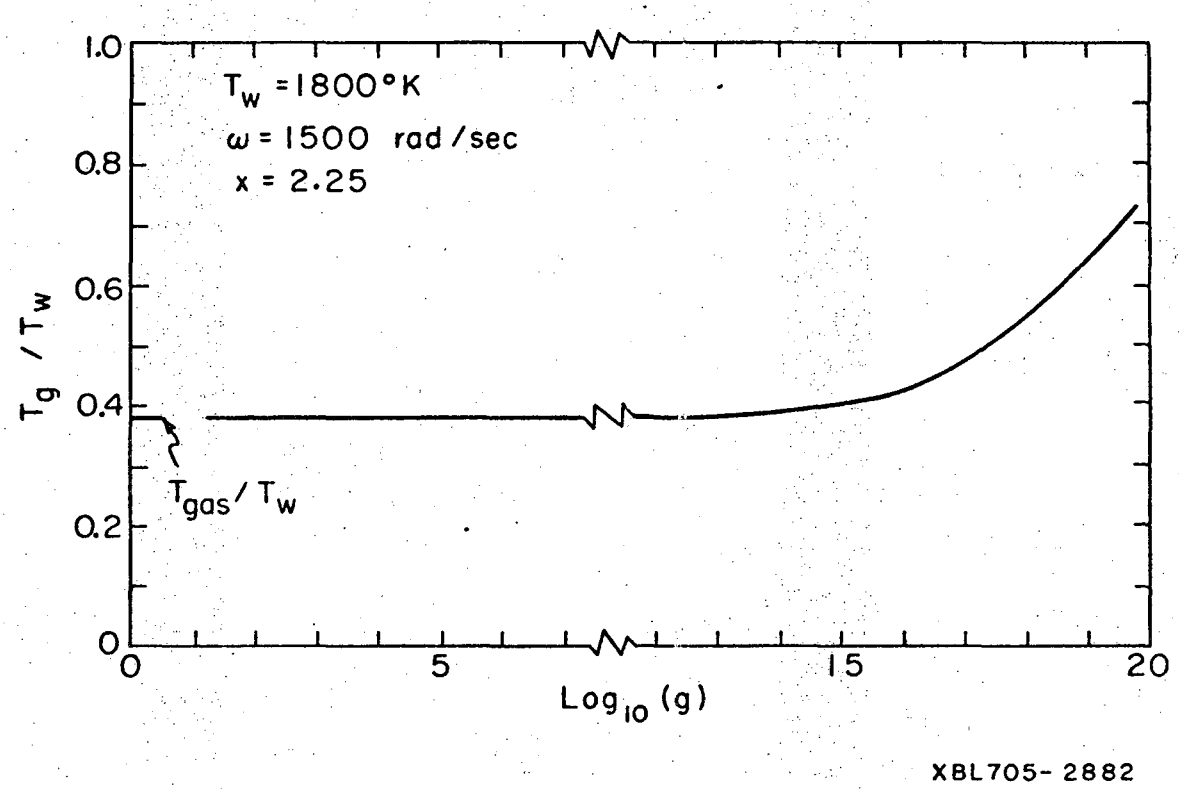

XBL705-2882

Fig. 9

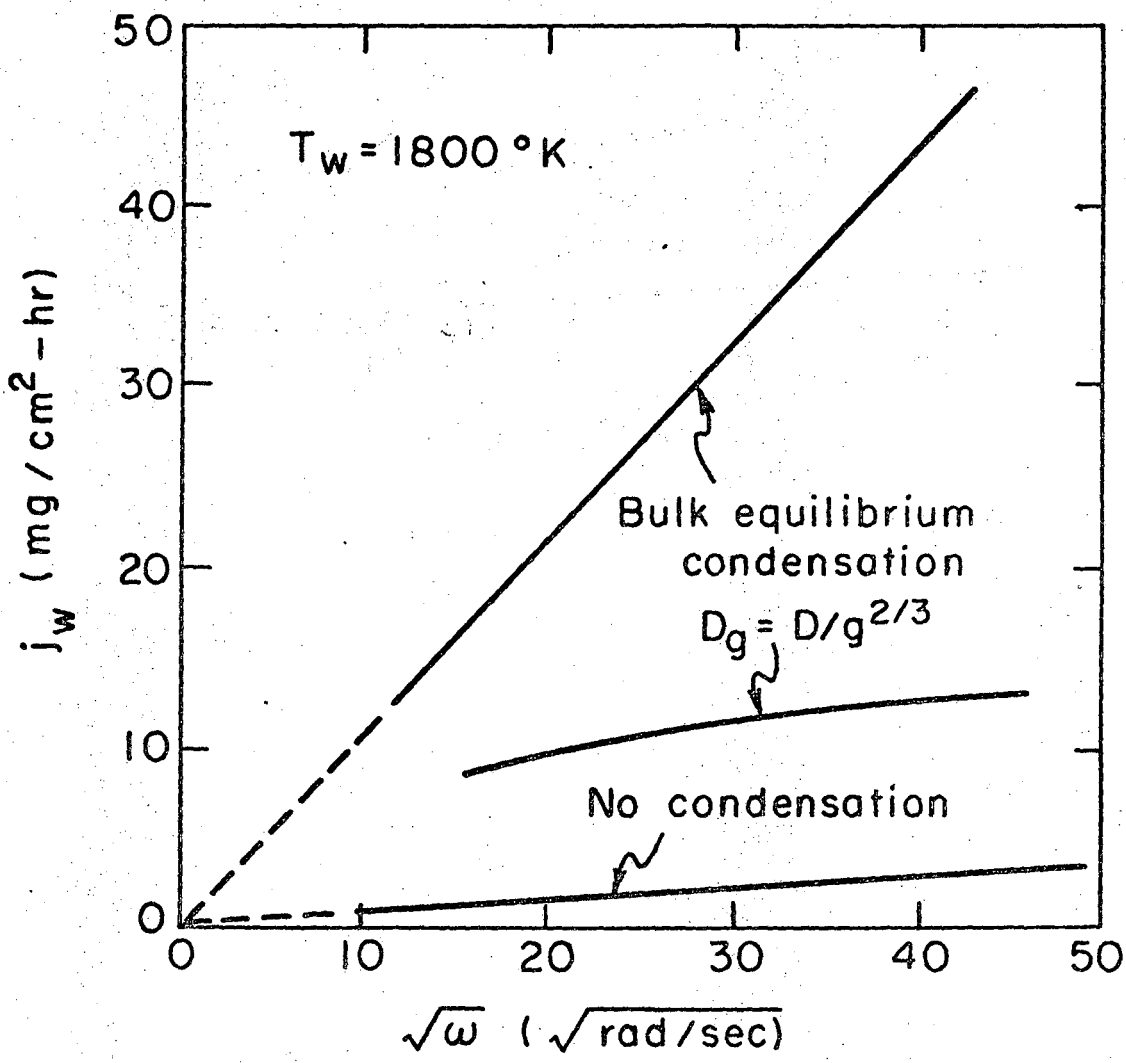

XBL705-2883

Fig. 10

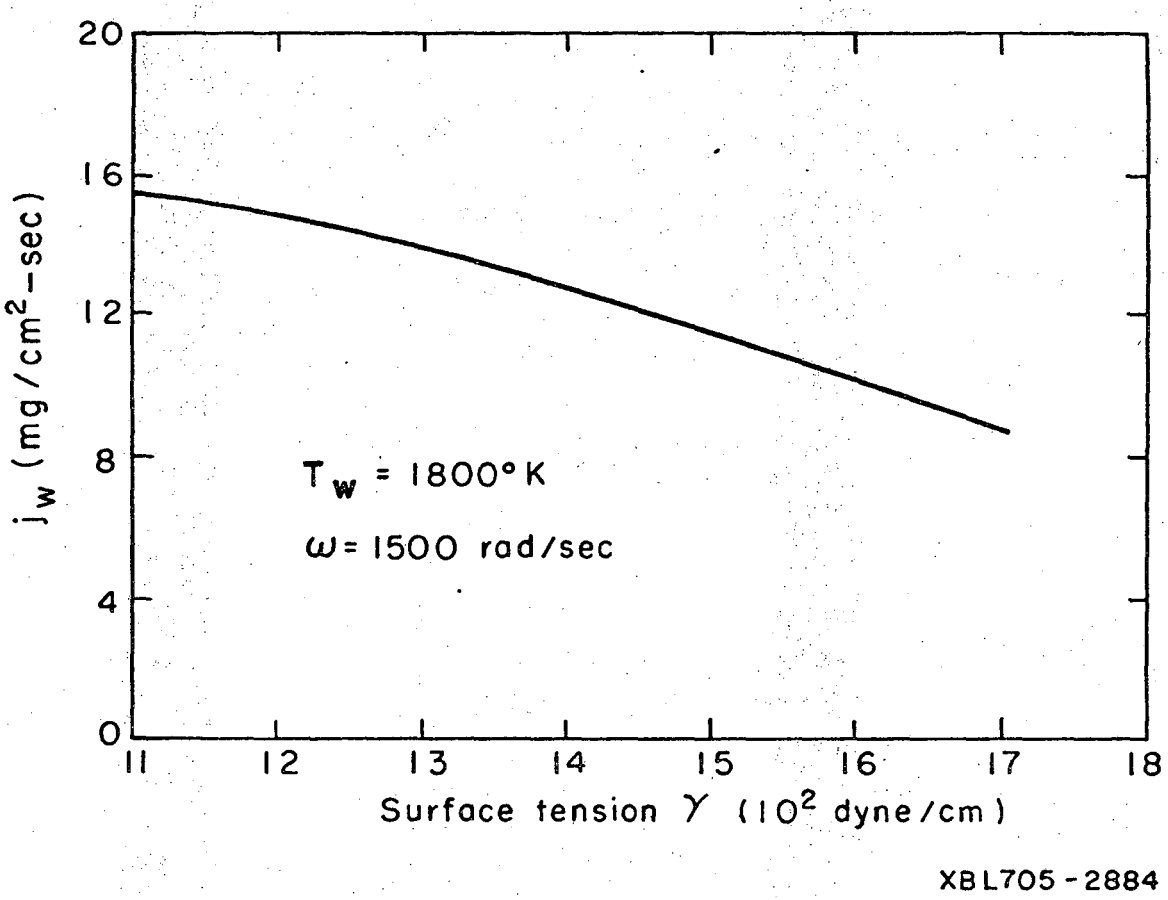
20
16
12
8
4
0
11
12
13
14
15
16
17
18
j_w (mg/cm^2-sec)
Surface tension γ (10^2 dyne/cm)
T_w = 1800° K
ω = 1500 rad/sec
XBL705-2884

Fig. 11

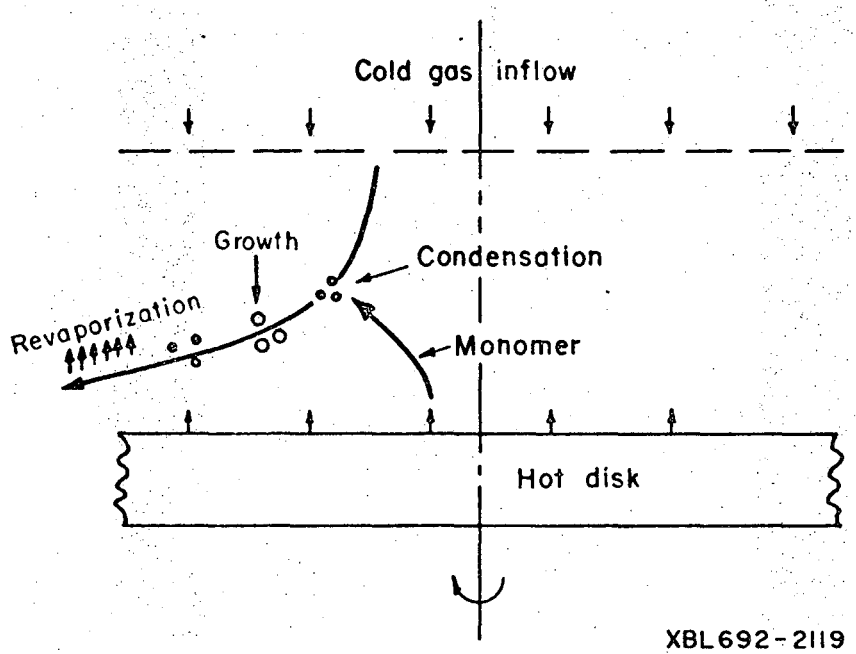
Cold gas inflow
Growth
Condensation
Revaporization
Monomer
Hot disk
XBL692-2119

Fig. 12

LEGAL NOTICE

This report was prepared as an account of Government sponsored work. Neither the United States, nor the Commission, nor any person acting on behalf of the Commission:

A. Makes any warranty or representation, expressed or implied, with respect to the accuracy, completeness, or usefulness of the information contained in this report, or that the use of any information, apparatus, method, or process disclosed in this report may not infringe privately owned rights; or

B. Assumes any liabilities with respect to the use of, or for damages resulting from the use of any information, apparatus, method, or process disclosed in this report.

As used in the above, "person acting on behalf of the Commission" includes any employee or contractor of the Commission, or employee of such contractor, to the extent that such employee or contractor of the Commission, or employee of such contractor prepares, disseminates, or provides access to, any information pursuant to his employment or contract with the Commission, or his employment with such contractor.

TECHNICAL INFORMATION DIVISION
LAWRENCE RADIATION LABORATORY
UNIVERSITY OF CALIFORNIA
BERKELEY, CALIFORNIA 94720